

Enzyme-Mediated Proximity Labeling Identifies Small RNAs in the Endoplasmic Reticulum Lumen

Ziqi Ren,[#] Ran Li,[#] Xinyue Zhou,[#] Yu Chen, Yuxin Fang, and Peng Zou*Cite This: *Biochemistry* 2023, 62, 1844–1848

Read Online

ACCESS |



Metrics & More



Article Recommendations



Supporting Information

ABSTRACT: In eukaryotic cells, the subcellular targeting of RNA controls many fundamental aspects of cellular physiology. Despite broad distributions throughout the cytoplasm, RNA molecules are conventionally believed to be excluded from the secretory pathway compartments including the endoplasmic reticulum (ER). Recent discovery of RNA *N*-glycan modification (glycoRNAs) has challenged this view, but direct evidence of RNA localization in the ER lumen has been lacking. In this study, we applied enzyme-mediated proximity labeling to profile the ER lumen-localized RNAs in human embryonic kidney 293T cells and rat cortical neurons. Our data set reveals the presence of small non-coding RNAs in the ER lumen, including U RNAs and Y RNAs, which raises interesting questions regarding their transport mechanism and biological functions in the ER.

The spatial organization of RNA in eukaryotic cells is intimately linked to gene expression regulation. RNA molecules have been found throughout cytoplasmic compartments, but direct evidence for their localization in the secretory compartments (e.g., endoplasmic reticulum) has been lacking. Recently, several small RNAs have been reported to be covalently modified with sialylated *N*-glycans (glycoRNAs) in mammalian cells.¹ Since the protein machineries required for *N*-glycosylation are thought to be exclusively localized within the endoplasmic reticulum (ER) lumen,^{2,3} it can be speculated that glycoRNAs may have been exposed to the ER lumen through a yet unknown transport mechanism. In addition, enrichment of cell surface biomolecules with nanoparticles has identified the presence of nuclear-coding RNAs on the extracellular side of mammalian cells.⁴ Other work also reported finding of cell-membrane-associated RNAs through APEX2-mediated proximity labeling.⁵ Altogether, the above evidence raises the interesting question of whether RNA molecules exist in the endoplasmic reticulum (ER) and whether they co-traffic with proteins in the secretory pathway. An unbiased transcriptome profiling in the ER lumen could yield an inventory of RNAs undergoing membrane translocation, which may shed light on their targeting mechanism.

Enzyme-mediated proximity labeling methods are powerful tools for analyzing the subcellular distribution of biological macromolecules in the context of live cells. For example, the engineered peroxidase APEX2 could convert the biotin-phenol (BP) substrate into a reactive biotin-phenoxyl free radical,^{6,7} which then attacks the surrounding RNAs by forming a covalent linkage with the electron-rich guanosine base, thus tagging proximal RNAs with a biotin handle for subsequent affinity enrichment and sequence identification (APEX-seq).^{8,9} Recently, our lab has developed MERR APEX-seq, which enhanced the sensitivity of APEX-seq through the metabolic incorporation of electron-rich ribonucleoside analogues, such as 6-thioguanosine (*s*⁶G) or 4-thiouridine (*s*⁴U), into nascent RNAs, thus increasing their reactivity toward the biotin-

phenoxyl free radical.¹⁰ We have demonstrated the high spatial specificity of MERR APEX-seq in several membrane-associated compartments, including the mitochondrial matrix, the ER membrane, and the nuclear lamina.

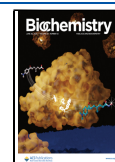
In this study, we sought to extend the MERR APEX-seq approach to profile RNAs in the ER lumen of cultured mammalian cells. We chose horseradish peroxidase (HRP) rather than APEX2 as the proximity labeling enzyme in the ER (i.e., MERR HRP-seq) for the following two reasons: (1) HRP is more active than APEX2 in the oxidizing environment of the ER lumen,¹¹ and (2) HRP is completely inactive in the reducing environment of cytoplasm, thus reducing background activity.^{7,12} We started with creating a human embryonic kidney 293T (HEK293T) cell line stably expressing HRP fused with the Ig κ signal sequence at its *N*-terminus and a tetra-amino acid ER-retention motif KDEL at its *C*-terminus (HRP-ER),¹¹ which together restrict HRP expression in the ER lumen. Considering that the diffusion of biotin-phenoxyl free radical might leak through the ER membrane (ERM) to label cytoplasmic RNAs, we separately created a HEK293T cell line expressing ERM-targeted, cytosol-facing APEX2 (APEX2-ERM) via fusion with the β subunit of the ER translocon complex Sec61, as the negative control.

We incubated HRP-ER and APEX2-ERM HEK293T cells with 100 μ M *s*⁶G for 5 h to metabolically incorporate the electron-rich ribonucleoside into newly transcribed RNAs and biotinylated by HRP in the presence of 0.5 mM biotin-phenol (BP) and 1 mM H₂O₂ treatment for 1 min (Figure 1A). Immunofluorescence microscopy confirms that the biotinyla-

Received: March 14, 2023

Revised: May 15, 2023

Published: May 30, 2023



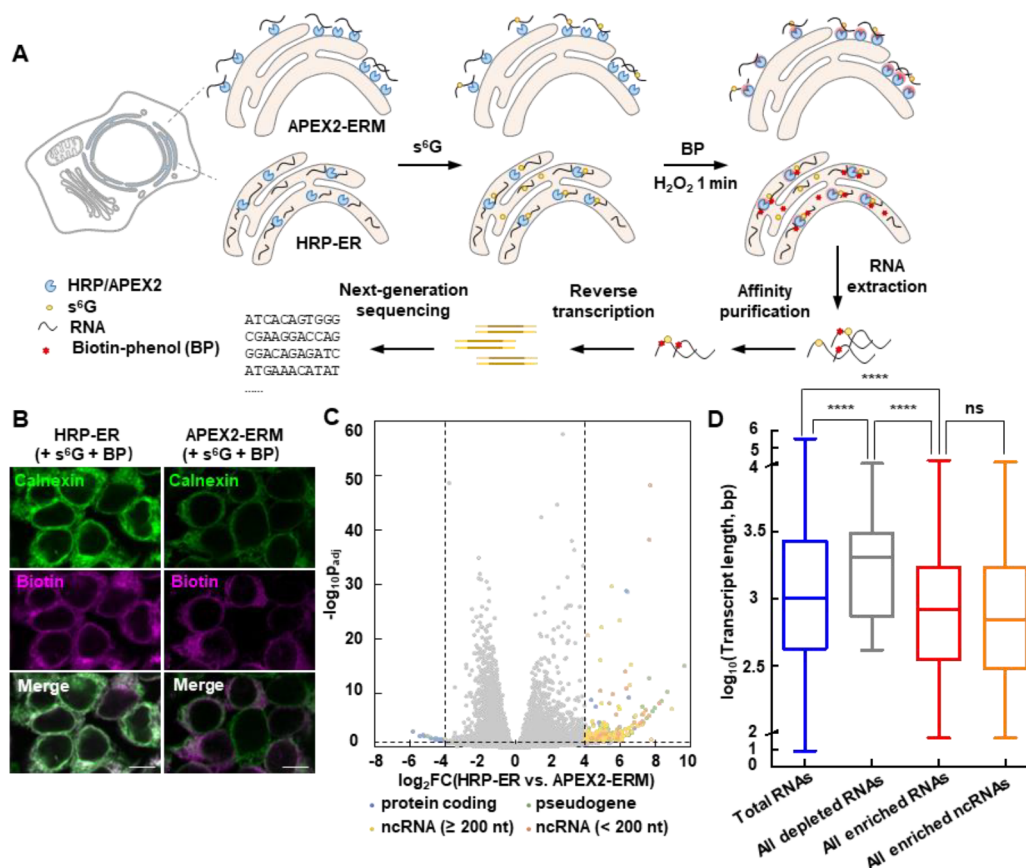


Figure 1. Profiling ER lumen transcriptome with proximity labeling. (A) Schematic of the MERR HRP/APEX-seq workflow. Cells are incubated with $100 \mu\text{M}$ s^6G for 5 h and labeled with 0.5 mM BP and 1 mM H_2O_2 . Biotinylated RNAs are enriched by streptavidin beads and analyzed by next-generation sequencing. (B) Immunofluorescence microscopy of HEK293T stably expressing HRP-ER (left) and APEX2-ERM (right). Green, antibody staining of ER marker calnexin; magenta, streptavidin staining of biotinylation. Scale bars: $10 \mu\text{m}$. (C) A volcano plot comparing the abundance of RNAs captured with HRP-ER vs APEX2-ERM labeling in HEK293T cells. (D) Box plot comparing the transcript length between total RNAs and enriched/depleted RNAs in DESeq2 analysis of HRP-ER vs APEX2-ERM. ns, not significant ($p > 0.05$); **** $p < 0.0001$ (Mann–Whitney test).

tion signal is highly co-localized with the ER marker, calnexin (Figure 1B). Following MERR HRP/APEX labeling, biotinylated RNAs were enriched by streptavidin-coated magnetic beads and analyzed by next-generation sequencing (Figure 1A). Enrichment of RNAs from each cell line is highly reproducible across biological replicates, with averaged Pearson's correlation coefficients ranging between 0.92 and 0.96 for HRP-ER (two replicates) and APEX2-ERM (four replicates) (Figure S1). Notably, the FPKM (fragments per kilobase per million reads) values of transcripts enriched from HRP-ER are quite distinct from those enriched from APEX2-ERM (Figure S2). For the HRP-ER samples, the averaged transcript FPKM values also appear substantially different between the input and the enriched (Figure S3), indicating the enrichment of a specific subpopulation of RNAs in the ER lumen.

We thus applied DESeq2¹³ analysis to compare the relative abundance of RNAs enriched from HRP-ER lumen labeling versus APEX2-ERM labeling. Beyond a cutoff of \log_2 Fold Change (HRP-ER vs APEX2-ERM) > 4 and adjusted p value < 0.05 , a total of 295 transcripts were enriched, including 35 mRNAs (12%), 96 pseudogenes (32%), and 164 non-coding RNAs (ncRNAs, 56%). In addition, 25 transcripts were depleted from the HRP-ER sample (i.e., selectively enriched in APEX2-ERM) beyond the cutoff of \log_2 Fold Change (HRP-

ER vs APEX2-ERM) < -4 and adjusted p value < 0.05 (Figure 1C, Supplementary Spreadsheet 1). We noted that the lengths of enriched RNAs in the ER lumen were significantly shorter than the total RNAs, with small RNAs (< 200 nt) constituting 16% in the enriched non-coding pool (Figure 1D, Supplementary Spreadsheet 1). Interestingly, in the list of 75 plasma-membrane-associated RNAs reported by Chen and co-workers, 29 are small RNAs.⁵ Meanwhile, the transcript lengths of depleted RNAs in the ER lumen are significantly longer than those of total RNAs (Figure 1D, Supplementary Spreadsheet 1). Together, the above evidence suggests that RNAs in the secretory pathway tend to have a shorter length than the total cellular RNA, and the enrichment of short ncRNAs in the ER lumen urged us to focus on identifying small RNAs in the ER lumen.

We repeated the HRP-ER lumen labeling with three biological replicates, with metabolic incorporation of $100 \mu\text{M}$ s^6G for 5 h followed by HRP-seq labeling with 0.5 mM BP and 1 mM H_2O_2 treatment. Following cell lysis and RNA extraction, small RNAs (< 200 nt) were isolated and further purified with streptavidin-coated beads (Figure 2A). Dot blot analysis confirmed the successful affinity purification of RNA molecules as the biotinylation signal of enriched samples was highly sensitive to RNase treatment but resistant to DNase or proteinase K (Figure 2B). We analyzed the length distribution

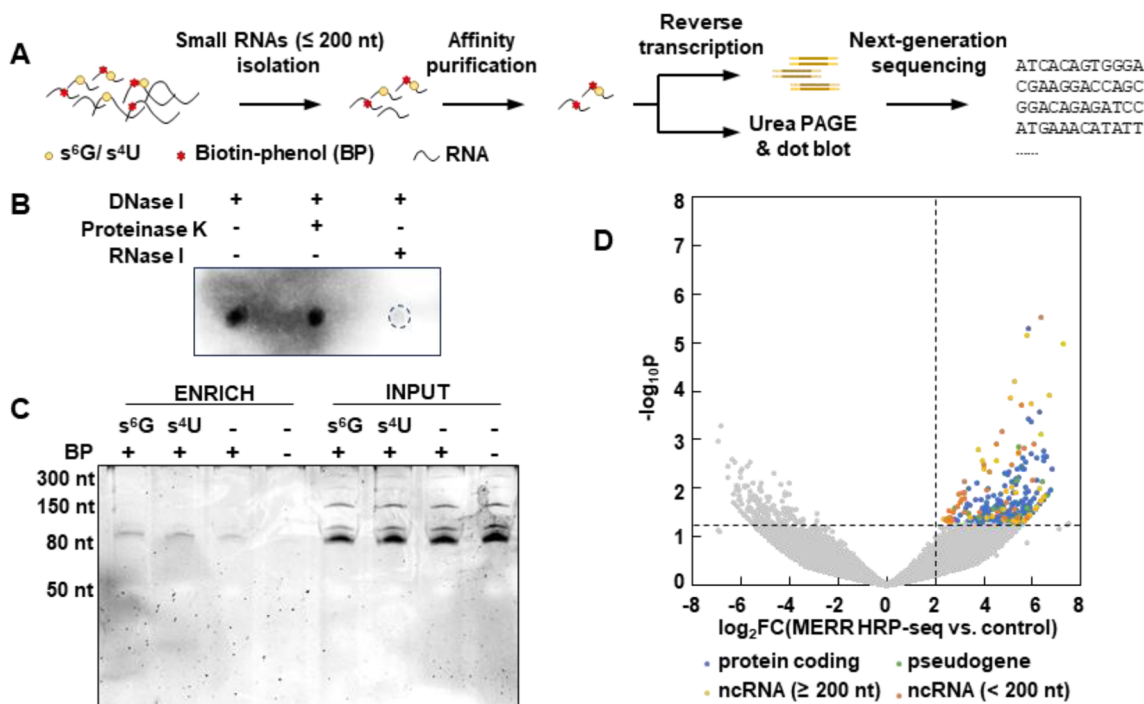


Figure 2. Profiling small RNAs in the ER lumen with MERR HRP-seq. (A) Schematic of the MERR HRP-seq workflow of profiling small RNAs in the ER lumen. (B) Dot blot analysis of enriched small RNAs treated with DNase I, proteinase K, or RNase I. (C) Urea PAGE analysis of the small RNA length distribution from HEK293T cells stably expressing HRP-ER before (INPUT) and after (ENRICH) affinity enrichment. (D) Volcano plot comparing the abundance of small RNAs captured in the ER lumen of HEK293T cells stably expressing HRP-ER.

of the post- and pre-enriched RNAs from different treated small RNAs samples through urea-PAGE. In parallel, we treated HRP-ER cells with either $100\ \mu\text{M}$ s^6G or s^4U for 5 h for metabolic incorporation to test the extensive feasibility of the enhanced labeling effect of MERR HRP/APEX-seq in detection of small RNAs. Urea PAGE analysis and SYBR Gold staining of enriched RNAs revealed the presence of an RNA band at approximately 80 nt (Figure 2C). When the HRP-ER cells were preincubated with either $100\ \mu\text{M}$ s^6G or s^4U , more biotinylated RNAs were enriched than control samples omitting metabolic incorporation (Figure 2C). Together, the above data demonstrated that HRP-ER labeling could capture small RNAs in the ER lumen with high sensitivity.

DESeq2 analysis comparing RNAs enriched from HRP-ER lumen labeling versus the negative control omitting the s^6G /BP probes revealed 76 significantly enriched ncRNAs ($\log_2\text{Fold Change} > 2$, p value < 0.05) (Figure 2D and Figure S4, Supplementary Spreadsheet 1). Among these, 22 RNAs were also present in our ER total RNA data set, including small RNAs like U RNAs, Y RNAs, snoRNAs, and vault RNAs (Table 1, Supplementary Spreadsheet 1 and Figure S5). Notably, in the work first describing RNA glycosylation,¹ Y RNAs were demonstrated to be highly enriched with their sialic acid based enrichment and sequencing,¹ implying that their presence in the ER lumen might be functionally linked to their glycosylation and transport to the cell membrane.

We further applied MERR HRP-seq to detect ER localized RNAs in cultured rat cortical neurons. At DIV3 (days *in vitro*), neurons were infected by lentivirus expressing HRP-ER driven by the human synapsin promoter (hSyn). MERR HRP-seq is performed on DIV9 (Figure 3A). Immunofluorescence microscopy showed good co-localization between the biotinylation signal and calnexin in the infected cells, whereas no

Table 1. List of ncRNAs Identified by MERR HRP-seq in the ER Lumen

Name	Type	Length (nt)	\log_2FC	
			HRP-ER vs APEX2-ERM	HRP-ER small RNA
AC007131.2	lnc RNA	1835	7.78	5.09
CTD-2651B20.7	lnc RNA	623	6.84	5.75
CTD-2651B20.6	lnc RNA	308	5.70	6.72
RNU5F-1	U RNA	117	4.83	2.95
RNU1-1	U RNA	164	6.30	2.57
RNU1-4	U RNA	164	5.57	3.17
RNU6ATAC	U RNA	126	5.00	2.60
RNU6-36P	U RNA	107	7.29	2.49
RNA5S9	5S rRNA	119	13.83	2.43
MIR4521	mi RNA	60	7.15	4.51
MT-TC	Mt tRNA	66	5.89	6.34
RNY1	Y RNA	113	5.41	2.45
RNY3	Y RNA	102	5.17	2.75
RNY4	Y RNA	96	7.29	2.91
VTRNA1-1	vault RNA	99	5.85	3.00
VTRNA1-2	vault RNA	89	6.79	4.00
VTRNA1-3	vault RNA	89	4.42	3.17
SNORA74A	sno RNA	198	4.32	2.60
SNORD13	sno RNA	104	7.49	3.83
SNORD3A	sno RNA	699	5.72	2.59
RN7SLSP	SRP RNA	321	5.52	3.76
RN7SL1	SRP RNA	299	4.87	2.35

biotinylation was observed in control cells omitting s^6G and BP (Figure 3B). Dot blot analysis confirmed the successful enrichment of biotinylated RNAs from labeled cortical neurons, while only low background was observed in negative

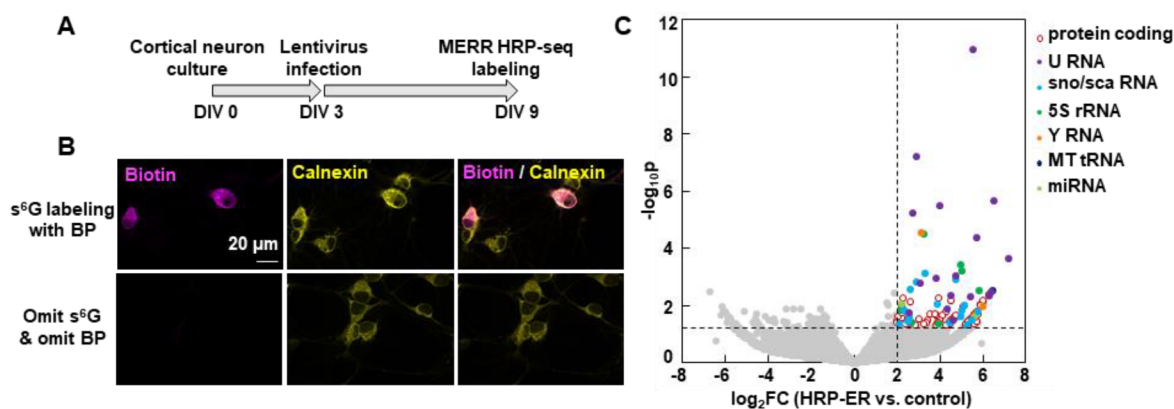


Figure 3. MERR HRP-seq profiling of small RNAs in the ER lumen of rat cortical neurons. (A) Scheme of MERR HRP-seq labeling in a rat cortical neuron. (B) Immunofluorescence microscopy of MERR HRP-seq labeled cortical neuron with infection of lentivirus composed of HRP-ER sequence. (C) Volcano plot comparing the abundance of small RNAs captured in the ER lumen of cortical neurons by MERR HRP-seq.

control samples, omitting HRP-ER expression (Figure S6). Following the same workflow of MERR HRP-seq in HEK293T cells, DESeq2 analysis identified 46 ncRNAs as significantly enriched above a cutoff of \log_2 Fold Change > 2.0 and p value < 0.05 (Figure 3C). All of the enriched ncRNAs were less than 328 bp with an average size of 147 bp, including 17 U RNA, 17 sno/sca RNA, and 2 Y RNA (Supplementary Spreadsheet 2). Notably, this inventory of enriched rat cortical neuronal RNAs is quite similar to those enriched from the ER lumen of cultured human cell lines, suggesting that the RNA targeting mechanism might be evolutionarily conserved.

To summarize, we have applied HRP-mediated proximity labeling to identify RNA molecules in the ER of cultured mammalian cells. The incorporation of electron-rich ribonucleoside enhanced the labeling sensitivity of HRP/APEX labeling, which allows us to discover low abundance transcripts in the ER lumen. In the labeling process, we chose 5 h incubation of s^6G and we speculated a shorter time could improve the time resolution of detecting nascent RNA but might lower the overall labeling yield. Our data reveal the existence of various types of small RNAs in the ER lumen, including Y RNAs that were previously reported to be glycosylated in mammalian cells. The existence of small RNAs in the ER lumen provides experimental support for RNA glycosylation in the secretory pathway.

It can be speculated from our findings that cytoplasmic RNAs could be transported across the ER membrane to enter the secretory pathway. However, the mechanism of RNAs translocating into the ER lumen has remained elusive. Notably, the concept of the transmembrane transport of RNA is not new. In the yeast mitochondria, tRNA has been reported to translocate across the inner mitochondrial membrane through the channels formed by the TOM (translocase of the outer mitochondrial membrane) and TIM (translocase of the inner mitochondrial membrane) complexes.¹⁴ In mammalian cells, lysosomal membrane protein SIDT2 can function as a transporter for RNA entry into lysosomes during RNautophagy.¹⁵ However, no RNA transporter has been identified on the ER membrane. Future genome-wide screening might help elucidate the mechanism of RNA translocation in the ER lumen and its trafficking along the secretory pathway.

It is noteworthy that our ER lumen MERR HRP-seq data set does not completely overlap with the reported list of glycoRNAs in H9 or HeLa cells.¹ For example, tRNAs have

been found in the list of glycoRNAs but missing from our data set. It is likely that our cDNA library construction workflow was not optimized for the detection of highly structured and modified tRNAs¹⁶ so that no reads from our cDNA library were mapped to the human mature tRNA.¹⁷ Notably, glycoRNAs were profiled by the metabolic labeling of sialic acid with an *N*-acetylmannosamine analogue, Ac₄ManNAz.¹ It is possible that certain RNAs in the ER lumen may be conjugated with other glycan forms lacking sialic acid or even are not substrates for glycosylation at all, which might explain their absence from the previous characterized glycoRNA inventory.

In conclusion, our data shed light on the fact that non-coding RNAs, particularly small RNAs, could exist in the ER lumen in both cultured mammalian cell lines and primary cells. It can be speculated from our findings that membrane localized RNAs could translocate to the cell membrane through the secretory pathway. The mechanism of translocation might be evolutionarily conserved, but the details have yet to be discovered.

■ ASSOCIATED CONTENT

Supporting Information

The Supporting Information is available free of charge at <https://pubs.acs.org/doi/10.1021/acs.biochem.3c00142>.

Key resource tables, Methods, and supplementary figures (PDF)

Supplementary Spreadsheet 1 including DESeq2 analysis in HEK293T (XLSX)

Supplementary Spreadsheet 2 including DESeq2 analysis in rat cortical neuron (XLSX)

■ AUTHOR INFORMATION

Corresponding Author

Peng Zou – College of Chemistry and Molecular Engineering, Synthetic and Functional Biomolecules Center, Beijing National Laboratory for Molecular Sciences, Key Laboratory of Bioorganic Chemistry and Molecular Engineering of Ministry of Education, Peking University, Beijing 100871, China; Academy for Advanced Interdisciplinary Studies, PKU-Tsinghua Center for Life Science and PKU-IDG/McGovern Institute for Brain Research, Peking University, Beijing 100871, China; Chinese Institute for Brain Research

(CIBR), Beijing 102206, China; orcid.org/0000-0002-9798-5242; Email: zoupeng@pku.edu.cn

Authors

Ziqi Ren – College of Chemistry and Molecular Engineering, Synthetic and Functional Biomolecules Center, Beijing National Laboratory for Molecular Sciences, Key Laboratory of Bioorganic Chemistry and Molecular Engineering of Ministry of Education, Peking University, Beijing 100871, China

Ran Li – Academy for Advanced Interdisciplinary Studies, PKU-Tsinghua Center for Life Science, Peking University, Beijing 100871, China

Xinyue Zhou – Academy for Advanced Interdisciplinary Studies, PKU-Tsinghua Center for Life Science, Peking University, Beijing 100871, China

Yu Chen – Academy for Advanced Interdisciplinary Studies, PKU-Tsinghua Center for Life Science, Peking University, Beijing 100871, China

Yuxin Fang – College of Chemistry and Molecular Engineering, Synthetic and Functional Biomolecules Center, Beijing National Laboratory for Molecular Sciences, Key Laboratory of Bioorganic Chemistry and Molecular Engineering of Ministry of Education, Peking University, Beijing 100871, China

Complete contact information is available at:

<https://pubs.acs.org/10.1021/acs.biochem.3c00142>

Author Contributions

#Z.R., R.L., X.Z.: Co-first authors.

Notes

The authors declare no competing financial interest.

ACKNOWLEDGMENTS

This work was supported by the Ministry of Science and Technology (2022YFA1304700, 2018YFA0507600) and the National Natural Science Foundation of China (32088101). P.Z. is sponsored by Bayer Investigator Award. The authors thank National Center for Protein Sciences at Peking University in Beijing, China, for assistance with Fragment Analyzer 12.

REFERENCES

- (1) Flynn, R. A.; et al. Small RNAs are modified with N-glycans and displayed on the surface of living cells. *Cell* **2021**, *184*, 3109–3124.
- (2) Schjoldager, K. T.; Narimatsu, Y.; Joshi, H. J.; Clausen, H. Global view of human protein glycosylation pathways and functions. *Nat. Rev. Mol. Cell Biol.* **2020**, *21*, 729–749.
- (3) Moremen, K. W.; Tiemeyer, M.; Nairn, A. V. Vertebrate protein glycosylation: diversity, synthesis and function. *Nat. Rev. Mol. Cell Biol.* **2012**, *13*, 448–462.
- (4) Huang, N.; et al. Natural display of nuclear-encoded RNA on the cell surface and its impact on cell interaction. *Genome Biol.* **2020**, *21*, 225.
- (5) Wu, E.; et al. Discovery of plasma membrane-associated RNAs through APEX-seq. *Cell Biochem. Biophys.* **2021**, *79*, 905–917.
- (6) Rhee, H.-W.; Zou, P.; Udeshi, N. D.; Martell, J. D.; Mootha, V. K.; Carr, S. A.; Ting, A. Y.; et al. Proteomic mapping of mitochondria in living cells via spatially restricted enzymatic tagging. *Science* **2013**, *339*, 1328–1331.
- (7) Lam, S. S.; et al. Directed evolution of APEX2 for electron microscopy and proximity labeling. *Nat. Methods* **2015**, *12*, 51–54.
- (8) Fazal, F. M.; et al. Atlas of subcellular RNA localization revealed by APEX-Seq. *Cell* **2019**, *178*, 473–490.

(9) Zhou, Y.; et al. Expanding APEX2 substrates for proximity-dependent labeling of nucleic acids and proteins in living cells. *Angew. Chem., Int. Ed.* **2019**, *58*, 11763–11767.

(10) Li, R.; Zou, Z.; Wang, W.; Zou, P. Metabolic incorporation of electron-rich ribonucleosides enhances APEX-seq for profiling spatially restricted nascent transcriptome. *Cell Chem. Biol.* **2022**, *29*, 1218–1231.

(11) Kaewsapsak, P. Live-cell mapping of organelle-associated RNAs via proximity biotinylation combined with protein-RNA crosslinking. *eLife* **2017**, *6*, e29224.

(12) Martell, J. D.; et al. Engineered ascorbate peroxidase as a genetically encoded reporter for electron microscopy. *Nat. Biotechnol.* **2012**, *30*, 1143–1148.

(13) Love, M. I.; Huber, W.; Anders, S. Moderated estimation of fold change and dispersion for RNA-seq data with DESeq2. *Genome Biol.* **2014**, *15*, 550.

(14) Salinas, T.; Duchêne, A.-M.; Maréchal-Drouard, L. Recent advances in tRNA mitochondrial import. *Trends Biochem. Sci.* **2008**, *33*, 320–329.

(15) Aizawa, S.; et al. Lysosomal putative RNA transporter SIDT2 mediates direct uptake of RNA by lysosomes. *Autophagy* **2016**, *12*, 565–578.

(16) Schaffer, A. E.; Pinkard, O.; Collier, J. M. tRNA Metabolism and Neurodevelopmental Disorders. *Annu. Rev. Genom. Hum. G.* **2019**, *20*, 359–387.

(17) Chan, P. P.; Lowe, T. M. GtRNAdb: a database of transfer RNA genes detected in genomic sequence. *Nucleic Acids Res.* **2009**, *37*, D93–D97.

Recommended by ACS

RNA Polymerase Ribozyme That Recognizes the Template-Primer Complex through Tertiary Interactions

Ankana Kakoti and Gerald F. Joyce

MAY 31, 2023
BIOCHEMISTRY

READ 

Site-Specific Covalent Labeling of DNA Substrates by an RNA Transglycosylase

Ember M. Tota and Neal K. Devaraj

MARCH 29, 2023
JOURNAL OF THE AMERICAN CHEMICAL SOCIETY

READ 

Deoxyguanosine-Linked Bifunctional Inhibitor of SAMHD1 dNTPase Activity and Nucleic Acid Binding

Matthew Egleston, James T. Stivers, et al.

MAY 26, 2023
ACS CHEMICAL BIOLOGY

READ 

The Transcriptome-Wide Mapping of 2-Methylthio-*N*⁶-isopentenyladenosine at Single-Base Resolution

Zhentian Fang, Xiang Zhou, et al.

FEBRUARY 23, 2023
JOURNAL OF THE AMERICAN CHEMICAL SOCIETY

READ 

Get More Suggestions >